# Exceptional points and dynamics of an asymmetric non-Hermitian two-level system

Sharad Joshi and Ian Galbraith
*Institute of Photonics and Quantum Sciences, SUPA, School of Engineering and Physical Sciences, Heriot-Watt University, Edinburgh EH14 4AS, United Kingdom*

(Received 13 July 2018; published 17 October 2018)

We investigated a damped two-level system interacting with a circularly polarized light as described by an asymmetric non-Hermitian Hamiltonian. This is a simple enough system to be studied analytically while complicated enough to exhibit a rich variety of behaviors. This system exhibits a ring of exceptional points in the parameter space of the real and imaginary dipole couplings where within the ring the energy eigenvalue of the system does not change. This leads to unstable regions inside the exceptional ring, which is shown using a linear stability analysis. These unstable regions are unique to gain-loss systems and have the surprising property that no matter how small the gain/loss ratio, the gain always prevails at long times. We also report on eigenvalue switching, phase rigidity and dynamics of the system around the exceptional points. We highlight that some of these properties are different from those in the widely studied case of symmetric non-Hermitian Hamiltonians.

DOI: 10.1103/PhysRevA.98.042117

## I. INTRODUCTION

The third postulate of quantum mechanics supposes that every physical observable has a corresponding quantum mechanical (QM) operator. From here, the usual conclusion is that these QM operators should be Hermitian, thereby leading to real eigenvalues and observables. Hermiticity is, however, only a sufficient condition to guarantee real observables. From such Hamiltonians, equations of motion for the observables (or the density matrix) can be derived and this master equation approach applies most naturally to closed quantum systems. A weaker condition is PT symmetry [1–3], where such Hamiltonians are non-Hermitian but retain a real eigenvalue spectrum. For open quantum systems interactions with the environment can be included by phenomenologically adding decays to these master equations with appropriate decay rates being separately estimated from the tunneling or scattering between system and reservoir. In contrast, non-Hermitian Hamiltonians incorporate the environment-system interaction by allowing the eigenvalues to be complex [4,5], where the imaginary part reflects the dissipation from the system to the environment [6,7]. The basic assumption of non-Hermitian formalism (a system embedded in a continuum of scattering wave functions to which the states of the system are coupled and into which they can decay) has been experimentally verified [8].

Examples that illustrate the utility of non-Hermitian quantum theory approaches include phase lapses in mesoscopic systems [9–11] where quantum phase transitions are experimentally observed in the transmission process in Aharonov-Bohm rings containing a quantum dot. This phenomenon can only be explained by considering from the start a non-Hermitian Hamiltonian [12] which demonstrates resonance trapping caused by feedback from the environment.

Another counterintuitive example is of dynamical phase transitions (DPTs). These are phase transitions observed in open quantum systems between nonanalytically connected states with respect to some external control parameter. These transitions are related to the existence of singular points in non-Hermitian formalism and cannot be explained by a Hermitian formalism. Near exceptional points, phase rigidity (see Sec. III) reduces and nonlinearities appear in the system, which leads to strong mixing of states [13]. In a two-level system this corresponds to width bifurcation in the vicinity of exceptional points while for a higher-level system this means a global spectroscopic redistribution takes place to dynamically stabilize the system. This results in one state (in a single-channel case) being strongly coupled to the environment while all other states are strongly decoupled from the environment [14,15] and is similar to Dicke superradiance in optics [16,17]. As reported in Ref. [14], Fermi's golden rule is violated in the vicinity of the exceptional point where a dynamical phase transition happens and is replaced by an anti–golden rule [17,18].

### Some aspects of non-Hermitian quantum mechanics

We now outline a few key properties of non-Hermitian quantum mechanics which we use in the rest of the paper. For a thorough introduction to non-Hermitian quantum mechanics please see Refs. [19,20].

In standard Hermitian quantum mechanics, orthogonality of the inner product ($\langle\phi_i|\phi_j\rangle = \delta_{i,j}$, where $|\phi_j\rangle$ are the right eigenvectors of the Hamiltonian) plays a central role in connecting operators to physical observables. In non-Hermitian quantum mechanics the definition needs to be generalized as the right eigenvectors no longer form an orthogonal basis. This generalised inner product is defined as $\langle\psi_i|\phi_j\rangle = \delta_{i,j}$, where $\langle\psi_i|$ are the left eigenvectors of the Hamiltonian. This formalism is based on biorthogonality, i.e., the orthogonal relationship between the eigenstates of the operator and its self-adjoint. This means the eigenstates of an operator are not necessarily orthogonal to each other but they are orthogonal to the states of the self-adjoint of the operator. This definition

 ©2018 American Physical Society

also facilitates a smooth transition between conventional quantum theory and non-Hermitian quantum mechanics in the limit of vanishing non-Hermiticity. A detailed derivation of the biorthogonal quantum mechanics formalism is presented in Ref. [21].

Degeneracy in Hermitian Hamiltonians is different than non-Hermitian degeneracy, where eigenvectors as well as eigenvalues coalesce at the degeneracy and thus provide an incomplete set of basis functions. The Hamiltonian at these non-Hermitian degeneracies is nondiagonalizable and known as a defective Hamiltonian in mathematics. These points in parameter space are called exceptional points after the pioneering work of Kato [22]. For specific parameter values, systems containing exceptional points (EPs) exhibit interesting physics including the divergent Petermann factor [23,24], loss-induced revival of lasing [25], single-mode lasers [26,27], dark-state lasers [28], coherent absorption [29], and unidirectional light propagation [30–32]. It has also been shown that in addition to the first-order pole in the Green's function due to the resonances, at the EP a second-order pole emerges due to the coalescence of eigenstates which leads to patterns resembling Fano-Feshbach resonances [33]. In an open quantum system embedded in the continuum of scattering wave functions it is possible for the states to couple via the environment thus causing the external mixing of states. The observable effects of such external mixing and associated non-Hermitian degeneracies on the resonance structure had been explored in two- and three-level systems [34]. It is shown that while the exceptional points do not influence the dynamics of an open quantum system in a one-channel case it does lead to observable effects for cases with two or more channels [34].

The topological properties of the exceptional points have been studied before [35]. It has been shown that by adiabatically encircling the exceptional point in parameter space the eigenvalues and eigenvectors can be permuted; i.e., the eigenvalues do not traverse in a closed curve in this case. This only happens when encircling the exceptional point.

All of the studies described above make use of symmetric ($H = H^{\mathrm{T}}$) non-Hermitian Hamiltonians. In this paper we investigate an open two-level system interacting with circularly polarized light which leads to an asymmetric non-Hermitian Hamiltonian. We find a ring of exceptional points in parameter space, phase jumps, and divergence of wave-vector coefficients in the natural basis at the exceptional point. We study the differences between a symmetric and asymmetric Hamiltonian with the same coupling intensity, particularly their dynamics and the stability of solutions in gain-loss systems. We also find that the definition of phase rigidity has to be modified to generalize to asymmetric Hamiltonians; i.e., the numerator should be replaced by the biorthogonal product.

## II. MODEL SYSTEM

The coherent time evolution of a two-level system under external perturbations can be described by the optical Bloch equations. There are many systems where the selection rule for excitation is $\Delta J_z = \pm 1$ and these transitions are driven by elliptically (or circularly) polarized light. We study a two-level system interacting with a circularly polarized light which can

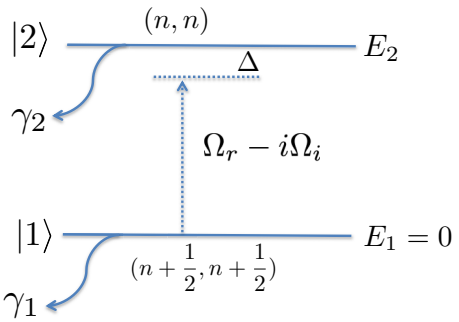


FIG. 1. Schematic of a two-level system interacting with left circularly polarized light ($\Omega_r - i\Omega_i$). Decays out of the system are captured by $\gamma_{1,2}$.

be described in the rotating frame by the Hamiltonian [36]

$$H_h = \hbar \begin{bmatrix} 0 & \Omega_r - i\Omega_i \\ \Omega_r + i\Omega_i & \Delta \end{bmatrix}, \tag{1}$$

where $\Delta$ is the detuning between the transition and laser energies and $\Omega_r$ and $\Omega_i$ are the real and imaginary parts of the dipole (Rabi) coupling. This Hamiltonian is self-adjoint, thus Hermitian, and therefore has real spectrum. Adding diagonal decay (or gain) to this Hamiltonian leads to an asymmetric non-Hermitian Hamiltonian,

$$H_{nh} = \hbar \begin{bmatrix} -i\gamma_1 & \Omega_r - i\Omega_i \\ \Omega_r + i\Omega_i & \Delta - i\gamma_2 \end{bmatrix}, \tag{2}$$

where $\gamma_1$ and $\gamma_2$ are the (positive or negative) interactions with the external bath as indicated in Fig. 1. The Bloch equations for this system can be derived as usual from the quantum Liouville equation as

$$\begin{bmatrix} \dot{n}_1 \\ \dot{n}_2 \\ \dot{P}_r \\ \dot{P}_i \end{bmatrix} = -\begin{bmatrix} 2\gamma_1 & 0 & 2\Omega_i & 2\Omega_r \\ 0 & 2\gamma_2 & -2\Omega_i & -2\Omega_r \\ -\Omega_i & \Omega_i & \gamma_1+\gamma_2 & \Delta \\ -\Omega_r & \Omega_r & -\Delta & \gamma_1+\gamma_2 \end{bmatrix} \begin{bmatrix} n_1 \\ n_2 \\ P_r \\ P_i \end{bmatrix}, \tag{3}$$

where $n_{1(2)}$ are the populations in the ground and excited states and $P_{r(i)}$ are the real and imaginary parts of the polarization. The remaining terms are as defined in the Hamiltonian above. As expected, population decays appear in the diagonal elements of the equations of motion, in the same way as if they had been introduced phenomenologically. In contrast to the optical Bloch equations with linearly polarized light, we see that both the real and imaginary parts of the polarization directly drive the populations.

We now explore the exceptional points and excitation dynamics of $H_{nh}$ and make comparisons with symmetric cases.

## III. EXCEPTIONAL RING AND PHASE RIGIDITY

The eigenvalues of $H_{nh}$ are complex and given by

$$\epsilon^{\pm} = \frac{\Delta - i(\gamma_1+\gamma_2)}{2} \pm \frac{\sqrt{(\Delta - i(\gamma_2-\gamma_1))^2 + 4\left(\Omega_r^2+\Omega_i^2\right)}}{2}. \tag{4}$$

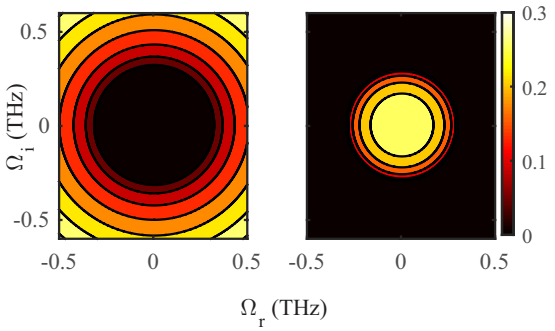


FIG. 2. Real (left) and imaginary (right) parts of one of the eigenvalues of $H_{nh}$ plotted in $(\Omega_r, \Omega_i)$ parameter space with $\Delta = 0$ THz and $\gamma_1 = 0.3$ THz and $\gamma_2 = -0.3$ THz. We can clearly see the exceptional ring at $|\Omega| = (\gamma_2 - \gamma_1)/2$.

Exceptional points arise for parameters for which the term under the square root goes to zero, i.e.,

$$\Delta = 0 \quad \text{and} \quad \Omega_r^2 + \Omega_i^2 = \frac{(\gamma_2 - \gamma_1)^2}{4}. \tag{5}$$

These conditions correspond to on-resonance excitation and a matching of the optical Rabi coupling ($\Omega$) and the differential gain/loss rate from the two levels. For these parameter values, the two eigenvectors coalesce into each other and the matrix is nondiagonalizable, having only one eigenvector. For a fixed $\gamma_1$ and $\gamma_2$ Eq. (5) describes a circle in the $(\Omega_r, \Omega_i)$ parameter space of radius $|\gamma_2 - \gamma_1|/2$, also known as an exceptional ring. Figure 2 shows that inside the ring the real part of the eigenvalues is zero but the imaginary part varies, while outside the ring the imaginary part is constant and the real part varies, consistent with Eqs. (4) and (5).

One of the interesting properties of exceptional points is that encircling the exceptional point once, in a three-dimensional parameter space $(\Delta, \Omega_r, \Omega_i)$ with either $\Omega_r$ or $\Omega_i$ fixed, leads to the swapping of eigenvalues. This is due to the fact that the instantaneous eigenbasis of non-Hermitian systems is not single valued when there is an exceptional point inside the loop [37].

At every fixed value of $(\Omega_r, \Omega_i)$, $H_{nh}$ has two exceptional points depending on whether $\gamma_2 - \gamma_1$ is positive or negative. The eigenvectors at these two exceptional points are given by $V_{nh}$:

$$V_{nh} = \frac{1}{\sqrt{2}} \begin{bmatrix} \pm \frac{(\Omega_i + i\Omega_r)}{\sqrt{\Omega_r^2 + \Omega_i^2}} \\ 1 \end{bmatrix}. \tag{6}$$

It has been shown that any real symmetric two-level system will have chiral eigenvalues [38], at the exceptional point, of the form

$$V_h = \frac{1}{\sqrt{2}} \begin{bmatrix} \pm i \\ 1 \end{bmatrix}. \tag{7}$$

We notice that while $V_{nh}$ depends on the ellipticity of the light, $V_h$ is independent of that. This parameter independence of the eigenvector is a property of any symmetric non-Hermitian two-level system. $V_{nh}$ becomes equivalent to $V_h$ when $\Omega_i = 0$ THz as the Hamiltonian becomes symmetric in this case.

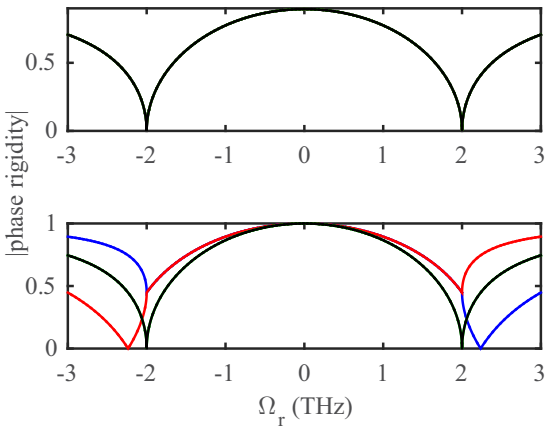


FIG. 3. The phase rigidity for $H'_{nh}$ (top) and for $H_{nh}$ (bottom). Parameters are $\Omega_i = 1$ THz, $\gamma_2 = 4.4721$ THz, and $\gamma_1 = 0$ THz. The exceptional points are at $\Omega_r = \pm 2$ THz. The phase rigidity in red and blue is calculated using each eigenvector using Eq. (9). The phase rigidity in black is calculated using a biorthogonal product definition of phase rigidity [Eq. (8)]. The figure is explained in the text below.

Far from an exceptional point, the states are almost orthogonal but as the states approach the exceptional point they become increasingly linearly dependent and hence their relative phase changes. This property is quantitatively defined by the phase rigidity,

$$r_i = \frac{\langle \psi_i | \phi_i \rangle}{\langle \psi_i^* | \phi_i \rangle}, \quad 0 < r_i < 1, \tag{8}$$

which measures the ratio of the $c$-product and inner product of a wave function. This ratio can be used to pinpoint the location of exceptional points in a system as it tends to zero as the system approaches the exceptional points. We can see that $r_i = 1$ everywhere for Hermitian systems. In Ref. [14], the analytical and numerical results of eigenfunctions and eigenvalues of a non-Hermitian Hamiltonian, phase rigidity, biorthogonality, and the influence of exceptional points on physical observables are discussed. For symmetric (non-Hermitian) systems the conventional definition of phase rigidity is

$$r_i = \frac{\langle \phi_i^* | \phi_i \rangle}{\langle \phi_i | \phi_i \rangle}, \quad 0 < r_i < 1. \tag{9}$$

We now compare the two phase-rigidity measures, Eqs. (8) and (9), for $H_{nh}$ [Eq. (2)] and a comparator-symmetrized version, namely,

$$H'_{nh} = \hbar \begin{bmatrix} -i\gamma_1 & |\Omega_r - i\Omega_i| \\ |\Omega_r + i\Omega_i| & \Delta - i\gamma_2 \end{bmatrix}. \tag{10}$$

This Hamiltonian has exactly the same energy spectrum as $H_{nh}$; i.e., the eigenvalues and EPs are identical in parameter space. As $H'_{nh}$ is symmetric its eigenvectors correspond to $V_h$ in Eq. (7) at the EP.

As can be seen in the upper panel of Fig. 3, both definitions (as expected) produce identical results for symmetric Hamiltonians with all curves precisely overlapping. In the lower panel, we can see that the biorthogonal product definition of phase rigidity [Eq. (8)] leads to the correct calculation of phase rigidity and thereby correctly identifies the EP location

at $\Omega_r = \pm 2$ THz. In contrast the original definition [Eq. (9)] leads to an incorrect identification of the EP as well as asymmetry when calculated using each eigenvector. In the symmetric case, the phase rigidity as defined in Eq. (9) reaches zero when $\Omega_r = \gamma_2/2$; i.e., it in effect ignores the contribution of $\Omega_i$ thus failing to correctly identify the exceptional points in the system. The asymmetric nature of phase rigidity (blue and red) in the lower panel of Fig. 3 is due to the asymmetry of the Hamiltonian which leads to different relationships among the eigenvectors for parameters in between and outside the exceptional points ($\pm 2$ THz). Between the exceptional points the eigenvectors are complex conjugate of each other, thus leading to an identical measure of phase rigidity. Outside the exceptional point region, the eigenvectors are different and not conjugate pairs which leads to different behavior on either side of the exceptional points. This problem does not arise for symmetric Hamiltonians as can be seen from the upper panel in Fig. 3. We conclude that the biorthogonality-based definition of phase rigidity [Eq. (9)] works well in all cases and is an appropriate metric for the identification of EPs.

## IV. DYNAMICS

In this section, we present the effects of the exceptional ring on the dynamics and stability of the system.

### A. Comparison between symmetric and asymmetric systems

We first compare the dynamics produced by $H_{nh}$ and $H'_{nh}$, two systems with identical spectra and EPs with potentially different dynamics induced by the asymmetric nature of the coupling in $H_{nh}$. From $H'_{nh}$ we obtain the Bloch equations,

$$\begin{bmatrix} \dot{n}'_1 \\ \dot{n}'_2 \\ \dot{P}'_r \\ \dot{P}'_i \end{bmatrix} = - \begin{bmatrix} 2\gamma_1 & 0 & 0 & 2|\Omega| \\ 0 & 2\gamma_2 & 0 & -2|\Omega| \\ 0 & 0 & \gamma_1+\gamma_2 & \Delta \\ -|\Omega| & |\Omega| & -\Delta & \gamma_1+\gamma_2 \end{bmatrix} \begin{bmatrix} n'_1 \\ n'_2 \\ P'_r \\ P'_i \end{bmatrix}, \tag{11}$$

which should be compared to Eq. (3). We solve the Bloch equations numerically in both cases. The dynamics are shown in Fig. 4 and clearly the dynamics of both Hamiltonians are different even though they have the same eigenvalues. This difference arises as the basis states for the two matrices are different even though their eigenspectra are identical. Interestingly, when the initial condition is [1 0] or [0 1], i.e., if we start with full population in one of the states, the dynamics are the same in both cases. The origin of this can be found by comparing the relevant Bloch equations of motion [Eqs. (3) and (11)] since for such initial conditions the driving terms are (and remain) identical.

### B. Instability ring

In this section we show the existence of an instability ring inside an exceptional ring in an optical gain-loss system. In this ring, however small the gain/loss ratio is, the system always runs away driven by the small gain. This has potential application in systems with high decay rates. We perform a linear stability analysis of the Schrödinger equation to find the instability ring in our system. For the non-Hermitian

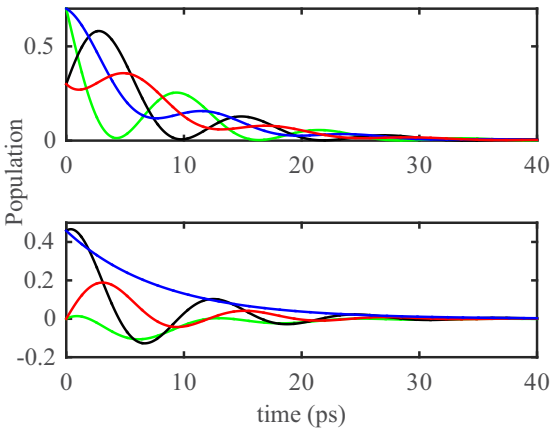


FIG. 4. Populations and polarization dynamics obtained from the solution of the Bloch equations for the initial conditions ($n_1 = 0.7$, $n_2 = 0.3$, $P_R = 0.4583$, $P_I = 0$). The parameters are $\Delta = 0$ THz, $\gamma_1 = 0.025$ THz, $\gamma_2 = 0.1$ THz, $\Omega_r = 0.08$ THz, and $\Omega_i = 0.25$ THz. Blue and red curves are for $H'_{nh}$ while green and black are for $H_{nh}$. Population in ground state (blue, black) and excited state (red, green). Polarization: real (blue, black) and imaginary (red, green).

Hamiltonian, $H_{nh}$ [Eq. (2)], expressing the dynamics in the eigenbasis we obtain for the amplitudes $C_1$ and $C_2$

$$\begin{bmatrix} \dot{C}_1 \\ \dot{C}_2 \end{bmatrix} = -i \begin{bmatrix} -i\gamma_1 & \Omega_r - i\Omega_i \\ \Omega_r + i\Omega_i & -i\gamma_2 \end{bmatrix} \begin{bmatrix} C_1 \\ C_2 \end{bmatrix}. \tag{12}$$

Since the Schrödinger equation is linear, the Jacobian can be written as

$$J = \begin{bmatrix} -\gamma_1 & -i\Omega_r - \Omega_i \\ -i\Omega_r + \Omega_i & -\gamma_2 \end{bmatrix},$$

and its eigenvalues are

$$\lambda^{\pm} = \frac{-(\gamma_1+\gamma_2)}{2} \pm \frac{\sqrt{(\gamma_2-\gamma_1)^2 - 4\left(\Omega_r^2 + \Omega_i^2\right)}}{2}. \tag{13}$$

For the system to be stable, all the eigenvalues of the Jacobian should be negative. Where at least one of the eigenvalues of the Jacobian is positive, i.e., when

$$\Omega_r^2 + \Omega_i^2 < -\gamma_1\gamma_2, \tag{14}$$

the solution will be unstable to small perturbations. For this inequality to be valid, $\gamma_1$ and $\gamma_2$ must have opposite signs; i.e., it should be a gain-loss system. So the instability ring exists only in a gain-loss system. This instability ring exists similarly in the symmetric Hamiltonian $H'_{nh}$ with $|\Omega|$ couplings and the stability condition remains the same as the asymmetric case.

Comparing Eq. (14) with the exceptional ring equality [Eq. (5)], we can see that the exceptional ring is always larger than the instability ring. Both rings exactly coincide when the system has balanced gain and loss ($\gamma_1 = -\gamma_2$). Figure 5 shows the ground-state population (the energy level connected to the sink) of the system inside and outside the instability ring. In this figure, the loss parameter ($\gamma_1$) is ten times greater than the gain parameter ($\gamma_2$). The instability ring in this case exists at $\Omega_r = 0.0316$ THz. We can see that inside the ring (blue) the state ends up gaining exponentially as time passes while for

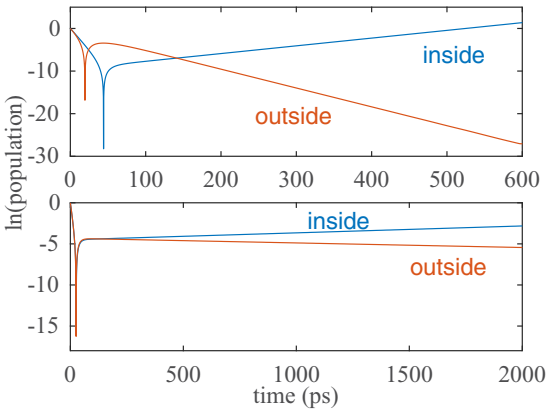


FIG. 5. Population of the ground state with time for a gain-loss system. The parameters are as follows: Initial condition $[C_1 = 1, C_2 = 0]$, $\Omega_i = 0.001$ THz, $\gamma_1 = 0.1$ THz, and $\gamma_2 = -0.01$ THz. The instability ring is at $\Omega_r = 0.0316$ THz. Top: Far inside the boundary of the stability ring ($\Omega_r = 0.01$ THz) and far outside the ring boundary ($\Omega_r = 0.05$ THz). Bottom: Close inside the boundary of the ring ($\Omega_r = 0.031$ THz) and just outside the ring ($\Omega_r = 0.032$ THz). Note the difference in time scales in upper and lower panels.

parameters outside the ring the system decays. We can also see that the farther we move inside the ring, the faster the gain rate is. This can be seen by comparing blue curves in the lower and upper panels. The lower panel shows that outside the ring the population decays exponentially with time. Here, too, the farther we move outside the ring, the faster the decay is. Thus even in a case such as this when the decay rate is ten times larger than the gain rate, the system can exhibit a runaway unstable behavior.

## V. EXPERIMENTAL VALIDATION

This system can be experimentally investigated using a two-level atom and circularly polarized light. Fixing $\Omega_r$ and setting $\Delta = 0$ THz, i.e., resonant excitation, and varying $\Omega_i$ within the exceptional ring (e.g., by changing the intensity of that component) will lead to no changes in the positions of the absorption spectrum peaks as the real parts of the eigenvalues do not change within the exceptional ring (see Fig. 2). The measured absorption peaks will get broadened, however, as the imaginary part of the eigenvalues do change within the exceptional ring. So small changes in intensity will not affect the spectrum until a critical value is reached. After that point, further increases will lead to splitting of the peaks but no further broadening as the real parts of the eigenvalues split outside the exceptional ring but the imaginary parts there become constant. Whether this is observable obviously depends on finding a system with sharp enough peaks to resolve the splitting. Another experiment might be encircling the exceptional point in $\Omega_r, \Delta$ space, i.e., intensity of light and the detuning space. Extracting the eigenvalues from the spectrum [39] generated by this experiment will show the switching of the eigenvalues.

## VI. CONCLUSIONS

We investigated a simple yet rich asymmetric non-Hermitian model system that can be experimentally verified using circularly polarized light interacting with a two-level system. We studied properties of phase rigidity and self-orthonormality and topological properties around the exceptional points. We showed, by comparing with similar symmetric non-Hermitian Hamiltonians, that, so long as the correct general definition of phase rigidity is used, it can always correctly identify the location of EPs. We also described an instability ring inside the exceptional ring where gain always wins regardless of a large loss channel present in the system. This has potential applications in systems with high decay rates because even a small gain can compensate for huge losses in the system, thus controlling the dynamics.

## ACKNOWLEDGMENT

S.J. acknowledges support from the EPSRC Centre for Doctoral Training in Condensed Matter Physics (Grant No. EP/L015110/1).

[1] C. M. Bender, Rep. Prog. Phys. **70**, 947 (2007).
[2] M. Znojil, SIGMA **5**, 001 (2009).
[3] A. Mostafazadeh, Int. J. Geom. Methods Mod. Phys. **7**, 1191 (2010).
[4] G. Gamow, Z. Phys. **51**, 204 (1928).
[5] A. J. Siegert, Phys. Rev. **56**, 750 (1939).
[6] I. Rotter, Rep. Prog. Phys. **54**, 635 (1991).
[7] I. Rotter, J. Phys. A: Math. Theor. **42**, 153001 (2009).
[8] Y. Yoon, M.-G. Kang, T. Morimoto, M. Kida, N. Aoki, J. L. Reno, Y. Ochiai, L. Mourokh, J. Fransson, and J. P. Bird, Phys. Rev. X **2**, 021003 (2012).
[9] M. Avinun-kalish, M. Heiblum, O. Zarchin, D. Mahalu, and V. Umansky, Nature (London) **436**, 529 (2005).
[10] C. Karrasch, T. Hecht, A. Weichselbaum, J. von Delft, Y. Oreg, and V. Meden, New J. Phys. **9**, 123 (2007).
[11] G. Hackenbroich, Phys. Rep. **343**, 463 (2001).
[12] M. Müller and I. Rotter, Phys. Rev. A **80**, 042705 (2009).
[13] I. Rotter and J. Bird, Rep. Prog. Phys. **78**, 114001 (2015).
[14] H. Eleuch and I. Rotter, Eur. Phys. J. D **69**, 229 (2015).
[15] H. Eleuch, Eur. Phys. J. D **69**, 230 (2015).
[16] R. H. Dicke, Phys. Rev. **93**, 99 (1954).
[17] H. Eleuch and I. Rotter, Eur. Phys. J. D **68**, 74 (2014).
[18] H. M. Pastawski, Physica B **398**, 278 (2007).
[19] N. Moiseyev, *Non-Hermitian Quantum Mechanics* (Cambridge University Press, Cambridge, UK, 2011).
[20] K. G. Zloshchastiev and A. Sergi, J. Mod. Opt. **61**, 1298 (2014).
[21] D. C. Brody, J. Phys. A: Math. Theor. **47**, 035305 (2013).
[22] T. Kato, *Perturbation Theory for Linear Operators*, Grundlehren der mathematischen Wissenschaften Vol. 132 (Springer-Verlag, Berlin, 1966).

[23] S.-Y. Lee, J.-W. Ryu, J.-B. Shim, S.-B. Lee, S. W. Kim, and K. An, Phys. Rev. A **78**, 015805 (2008).
[24] A. M. van der Lee, N. J. van Druten, A. L. Mieremet, M. A. van Eijkelenborg, Å. M. Lindberg, M. P. van Exter, and J. P. Woerdman, Phys. Rev. Lett. **79**, 4357 (1997).
[25] B. Peng, Ş. Özdemir, S. Rotter, H. Yilmaz, M. Liertzer, F. Monifi, C. Bender, F. Nori, and L. Yang, Science **346**, 328 (2014).
[26] L. Feng, Z. J. Wong, R.-M. Ma, Y. Wang, and X. Zhang, Science **346**, 972 (2014).
[27] H. Hodaei, M.-A. Miri, M. Heinrich, D. N. Christodoulides, and M. Khajavikhan, Science **346**, 975 (2014).
[28] H. Hodaei, A. Hassan, W. Hayenga, M. Miri, D. Christodoulides, and M. Khajavikhan, Opt. Lett. **41**, 3049 (2016).
[29] Y. Sun, W. Tan, H.-Q. Li, J. Li, and H. Chen, Phys. Rev. Lett. **112**, 143903 (2014).
[30] A. Guo, G. J. Salamo, D. Duchesne, R. Morandotti, M. Volatier-Ravat, V. Aimez, G. A. Siviloglou, and D. N. Christodoulides, Phys. Rev. Lett. **103**, 093902 (2009).
[31] Z. Lin, H. Ramezani, T. Eichelkraut, T. Kottos, H. Cao, and D. N. Christodoulides, Phys. Rev. Lett. **106**, 213901 (2011).
[32] L. Feng, Y.-L. Xu, W. S. Fegadolli, M.-H. Lu, J. E. Oliveira, V. R. Almeida, Y.-F. Chen, and A. Scherer, Nat. Mater. **12**, 108 (2013).
[33] W. D. Heiss and G. Wunner, Eur. Phys. J. D **68**, 284 (2014).
[34] H. Eleuch and I. Rotter, Phys. Rev. A **95**, 022117 (2017).
[35] D. Heiss, Nat. Phys. **12**, 823 (2016).
[36] G. Slavcheva and O. Hess, Phys. Rev. A **72**, 053804 (2005).
[37] R. Uzdin, A. Mailybaev, and N. Moiseyev, J. Phys. A: Math. Theor. **44**, 435302 (2011).
[38] W. Heiss and H. Harney, Eur. Phys. J. D **17**, 149 (2001).
[39] H. Cartarius, J. Main, and G. Wunner, Phys. Rev. Lett. **99**, 173003 (2007).